Electron trajectories and gain in a free-electron laser with realizable helical wiggler and ion-channel guiding

Madhi Esmaeilzadeh, Sadollah Ebrahimi, and Alaeddin Saiahian
Department of Physics, Iran University of Science and Technology, Tehran, Iran

Joseph E. Willett[a)]
Department of Physics & Astronomy, University of Missouri-Columbia, Columbia, Missouri 65211

Lori Jo Willett
Department of Mathematics, University of New Orleans, New Orleans, Louisiana 70148

A theory is developed for a free-electron laser (FEL) with a three-dimensional helical wiggler and ion-channel guiding. The relativistic equation of motion for a single electron in the combined wiggler and ion-channel fields is solved in the rotating wiggler frame. With the aid of the conservation of energy, equations for the axial velocity and the Φ function (which determines the rate of change of axial velocity with energy) are studied numerically. An analysis of the electromagnetic radiation copropagating with the electron beam in the FEL interaction region is also presented. The gain formula is derived and calculations indicate that the gain of the realizable wiggler is considerably greater than the gain of the idealized one, and the gain enhancement increases with increasing wiggler magnetic field. It is shown that the gain for group-I orbits is positive, while for group-II orbits, the gain is negative in the negative mass regime (i.e., $\Phi < 0$) and positive in the positive mass regime. © *2005 American Institute of Physics.*
[DOI: 10.1063/1.2006690]

I. INTRODUCTION

A free-electron laser (FEL) is a high-intensity, continuously tunable source of coherent electromagnetic radiation. The radiation is generated by the passage of a relativistic electron beam through a static, spatially periodic magnetic field. The electron beam can be collimated by a uniform static axial magnetic field produced by the current in a solenoid. As an alternative to guiding the relativistic electron beam by use of an axial magnetic field, ion-channel guiding has been proposed.[1] This technique involves the creation of a plasma channel by passage of a uv-laser beam through a gas. The plasma electrons are then electrostatically repelled by injection of the relativistic electron beam through the channel. The resulting ion channel attracts and transversely confines the beam electrons. Theoretical studies of electron trajectories and gain in a helical-wiggler FEL with ion-channel guiding have been carried out by Jha and Kumar.[2,3] They were subsequently extended by Esmaeilzadeh *et al.*[4] Recently an analysis of trajectories in a helical wiggler with both an ion channel and a parallel/reversed axial magnetic field has been published.[5] Also, the effects of the self-fields in a helical wiggler have been investigated.[6,7]

All of the above cited analyses of an ion-channel FEL are based on a helical wiggler in an idealized one-dimensional approximation. In the present paper, a more realistic (realizable) helical wiggler is employed. In Sec. II, the relativistic equation of motion for a single electron in the combined realizable helical magnetic wiggler and electrostatic ion-channel fields is solved. The steady-state transverse velocity components are thereby obtained in the rotating wiggler frame. Next the conservation of energy is invoked to derive an equation for the axial velocity. The equation for the Φ function which determines the rate of change of axial velocity with energy is then derived. In Sec. III, the electromagnetic radiation copropagating with the electron beam in the FEL interaction region is analyzed. The self-consistent pendulum equation describing the electron-photon interaction in a realizable helical wiggler and ion channel is derived. Next an equation for the change of the electromagnetic power in one transit time through the wiggler interaction length is obtained. The gain equation for a FEL with realizable helical wiggler and ion channel is then derived. In Sec. IV, the results of a numerical study of the orbits and gain are presented. The axial velocity, the function Φ, and the gain have been computed as functions of the ion-channel frequency. Function Φ which determines the rate of change of axial velocity with energy and the gain factor due to the ion channel are shown as functions of the normalized ion-channel frequency for the stable branches of the group-I and group-II orbits. The normalized axial velocity is shown as a function of the normalized ion-channel frequency for both stable and unstable group-I and group-II orbits.

II. ELECTRON ORBITS AND FUNCTIONS Φ

A realizable (three-dimensional) helical wiggler, generated by bifilar current windings, may be described by[8–11]

---

a)Electronic mail: willettje@missouri.edu

$$\mathbf{B}_w = 2B_w[I_1'(\lambda)\hat{\mathbf{e}}_r \cos\chi - I_1(\lambda)(\lambda^{-1}\hat{\mathbf{e}}_\theta \sin\chi - \hat{\mathbf{e}}_z \sin\chi)] \tag{1}$$

in cylindrical coordinates, where B_w is the amplitude of the wiggler magnetic field, $\lambda \equiv k_w r$, $k_w \equiv 2\pi/\lambda_w$ is the wiggler period, $\chi \equiv \theta - k_w z$, and I_1, I_1' are the modified Bessel function of the first kind (of order 1) and its derivative, respectively. This field indicates a local minimum on the axis, i.e., at $r=0$, which acts to focus and to confine the beam against the effects of self-electric and magnetic fields generated by charge density and current of nonneutral electron beams.[8] However, for intense electron beams, a guiding field (e.g., an axial magnetic field) is often employed in conjunction with a helical wiggler in order to provide enhanced focusing.

In this paper, we use the transverse electrostatic field generated by an ion channel as a guiding field. The ion-channel electric field may be written as

$$\mathbf{E}_i = 2\pi e n_i r \hat{\mathbf{e}}_r, \tag{2}$$

where n_i is the density of positive ions having charge $+e$. The relativistic equation of motion for an electron with rest mass m and charge $-e$ moving with velocity $\mathbf{v}$ in the combined wiggler magnetic and ion-channel electric fields is

$$\frac{d(m\gamma\mathbf{v})}{dt} = -e\left(\mathbf{E}_i + \frac{1}{c}\mathbf{v}\times\mathbf{B}_w\right), \tag{3}$$

where γ is the relativistic factor, and c is the speed of light *in vacuo*. For convenience we work in the wiggler frame defined by basis vectors

$$\hat{\mathbf{e}}_1 = \hat{\mathbf{e}}_r \cos\chi - \hat{\mathbf{e}}_\theta \sin\chi, \tag{4}$$

$$\hat{\mathbf{e}}_2 = \hat{\mathbf{e}}_r \sin\chi + \hat{\mathbf{e}}_\theta \cos\chi, \tag{5}$$

$$\hat{\mathbf{e}}_3 = \hat{\mathbf{e}}_z. \tag{6}$$

In this frame, the scalar equations of motion for the steady-state orbits ($\gamma = \gamma_0 = $ const, $\dot{\gamma} = 0$) can be written as

$$\frac{d\beta_1}{dt} = -k_w c\{\bar{\omega}_i^2 \lambda \cos\chi + \beta_2[2\bar{\Omega}_w I_1(\lambda)\sin\chi - \beta_3]$$
$$- \beta_3 \bar{\Omega}_w I_2(\lambda)\sin(2\chi)\}, \tag{7}$$

$$\frac{d\beta_2}{dt} = -k_w c\{\bar{\omega}_i^2 \lambda \sin\chi - \beta_1[2\bar{\Omega}_w I_1(\lambda)\sin\chi - \beta_3]$$
$$+ \beta_3 \bar{\Omega}_w[I_0(\lambda) + I_2(\lambda)\cos(2\chi)]\}, \tag{8}$$

$$\frac{d\beta_3}{dt} = k_w c\bar{\Omega}_w\{\beta_2[I_0(\lambda) + I_2(\lambda)\cos(2\chi)]$$
$$- \beta_1 I_2(\lambda)\sin(2\chi)\}, \tag{9}$$

$$\frac{d\chi}{dt} = \frac{-k_w c}{\lambda}(\beta_1 \sin\chi - \beta_2 \cos\chi + \beta_3 \lambda), \tag{10}$$

$$\frac{d\lambda}{dt} = k_w c(\beta_1 \cos\chi + \beta_2 \sin\chi), \tag{11}$$

where $\beta_1 \equiv v_1/c$, $\beta_2 \equiv v_2/c$, $\beta_3 \equiv v_3/c$ are the components of the normalized velocity in the (rotating) wiggler frame, $\bar{\omega}_i \equiv (2\pi e^2 n_i/m\gamma k_w^2 c^2)^{1/2}$ is the normalized ion-channel frequency, and $\bar{\Omega}_w = eB_w/(m\gamma k_w c^2)$ is the normalized wiggler magnetic field. The steady-state solution in which β_1, β_2, β_3, χ, and λ are constants can be obtained in the form

$$\beta_1 \equiv \beta_w = \frac{2\Omega_w \beta_\parallel^2 I_1(\lambda_0)/\lambda_0}{\bar{\omega}_i^2 \pm 2\bar{\Omega}_w \beta_\parallel I_1(\lambda_0) - \beta_\parallel^2}, \tag{12}$$

where

$$\beta_2 = 0, \tag{13}$$

$$\beta_3 \equiv \beta_\parallel = \text{const}, \tag{14}$$

$$\chi = \pm \pi/2, \tag{15}$$

$$\lambda \equiv \lambda_0 = \mp \beta_w/\beta_\parallel, \tag{16}$$

and β_w is the wiggler-induced transverse velocity. In the limit $\lambda \to 0$, Eq. (12) reduces to

$$\beta_w^{\text{id}} = \frac{\bar{\Omega}_w \beta_\parallel^2}{\bar{\omega}_i^2 - \beta_\parallel^2} \tag{17}$$

which is the wiggler-induced transverse velocity for an idealized helical wiggler with ion-channel guiding.[2,4] Using Eqs. (14)–(16), the steady-state electron displacements in the wiggler frame can be obtained as

$$\chi_1 = \frac{\lambda_0 \cos\chi}{k_w} = 0, \tag{18}$$

$$\chi_2 = \frac{\lambda_0 \sin\chi}{k_w} = -\frac{2\bar{\Omega}_w \beta_\parallel I_1(\lambda_0)/\lambda_0}{k_w[\bar{\omega}_i^2 \pm 2\bar{\Omega}_w \beta_\parallel I_1(\lambda_0) - \beta_\parallel^2]}, \tag{19}$$

$$\chi_3 = c\beta_\parallel t. \tag{20}$$

Since the wiggler frame is a helical rotating frame, the electron trajectory is a perfect helix in the laboratory frame (x, y, z), with its axis coincident with the free-electron laser (z) axis. Equations (12) and (19) show resonant enhancement in magnitude of the transverse electron velocity and displacement when

$$\bar{\omega}_i^2 \pm 2\bar{\Omega}_w I_1(\lambda_0)\beta_\parallel - \beta_\parallel^2 = 0 \tag{21}$$

which separates the electron orbits into two groups. Groups I and II are defined by

$$\bar{\omega}_i < [\beta_\parallel^2 - 2\bar{\Omega}_w \beta_\parallel I_1(\lambda_0)]^{1/2} \tag{22}$$

and

$$\bar{\omega}_i > [\beta_\parallel^2 + 2\bar{\Omega}_w \beta_\parallel I_1(\lambda_0)]^{1/2}, \tag{23}$$

respectively. Complete determination of the steady-state orbits requires knowledge of β_1, $\beta_\parallel$, or λ_0; determination of any one of these is sufficient to calculate the other two. The

normalized axial velocity $\beta_\parallel$ can be determined from the conservation of energy using Eqs. (12) and (16). This yields

$$\beta_\parallel^2(\bar{\omega}_i^2 - \beta_\parallel^2) + (\gamma^{-2} - 1)\lfloor\bar{\omega}_i^2 \pm 2\bar{\Omega}_w\beta_\parallel I_1(\lambda_0) - \beta_\parallel^2\rfloor = 0, \quad (24)$$

where

$$\lambda_0 \equiv \mp \frac{1}{\beta_\parallel}(\gamma_\parallel^{-2} - \gamma^{-2})^{1/2}, \quad (25)$$

and

$$\gamma_\parallel \equiv (1 - \beta_\parallel^2)^{-1/2}. \quad (26)$$

In Eq. (25), $-(+)$ corresponds to $\beta_\parallel < 0(\beta_\parallel > 0)$. Since Eq. (24) is symmetric in $\beta_\parallel$, it yields orbits that are independent of the direction of electron propagation. Here, we consider only forward propagation (i.e., $\beta_\parallel > 0$).

Implicit differentiation of Eq. (24) yields

$$\frac{d\beta_\parallel}{d\gamma} = \frac{1}{\gamma\gamma_\parallel^2\beta_\parallel}\Phi, \quad (27)$$

where

$$\Phi \equiv 1 - \frac{\beta_\parallel^2\lambda_0^2(1 + \gamma_\parallel^2) \pm P(\lambda_0)\beta_\parallel^{-3}\lambda_0(1 + \gamma^{-2} + 2\gamma_\parallel^2) + Q(\lambda_0)(\gamma_\parallel^2 - \gamma^2)}{2(\bar{\omega}_i^2 - \beta_\parallel^2) + (\gamma^{-2} - 1)[\gamma^2 Q(\lambda_0) \pm P(\lambda_0)\beta_\parallel^{-3}\lambda_0] + 2\beta_\parallel^2\lambda_0^2}. \quad (28)$$

In Eq. (28), P and Q are defined by

$$P \equiv 2\bar{\Omega}_w\beta_\parallel^2 I_1(\lambda_0)/\lambda_0 \quad (29)$$

and

$$Q \equiv \frac{\pm 2(\gamma^{-2} - 1)\bar{\Omega}_w I_1'(\lambda_0)}{\lambda_0\beta_\parallel^3\gamma^2}, \quad (30)$$

respectively. The function Φ is used to determine the mass regimes, which are used to describe the negative and positive gains.

III. STABILITY OF ELECTRON ORBITS

The stability of the steady-state orbits can be determined by considering small perturbations about the steady-state orbits: $\beta_1 = \beta_w + \delta\beta_1$, $\beta_2 = \delta\beta_2$, $\beta_3 = \beta_\parallel + \delta\beta_3$, $\chi = \pm\pi/2 + \delta\chi$, $\lambda = \lambda_0 + \delta\lambda$, and $\gamma = \gamma_0 + \delta\gamma$. Considering energy exchange of the electron with the electrostatic field, the orbit equations after expanding to the first order in the perturbed variables can be written as

$$\delta\dot{\beta}_1 = \alpha_{12}\delta\beta_2 + \alpha_{14}\delta\chi, \quad (31)$$

$$\delta\dot{\beta}_2 = \alpha_{21}\delta\beta_1 + \alpha_{23}\delta\beta_3 + \alpha_{25}\delta\lambda + \alpha_{26}\delta\gamma, \quad (32)$$

$$\delta\dot{\beta}_3 = \alpha_{32}\delta\beta_2 + \alpha_{34}\delta\chi, \quad (33)$$

$$\delta\dot{x} = \alpha_{41}\delta\beta_1 + \alpha_{43}\delta\beta_3 + \alpha_{45}\delta\lambda, \quad (34)$$

$$\delta\dot{\lambda} = \alpha_{52}\delta\beta_2 + \alpha_{54}\delta\chi, \quad (35)$$

$$\delta\dot{\gamma} = \alpha_{62}\delta\beta_2 + \alpha_{64}\delta\chi, \quad (36)$$

where dot indicates d/dt. The last equation is derived from

$$\dot{\gamma} = -\frac{e}{mc^3}\bar{\beta}\cdot\mathbf{E}_i \quad (37)$$

which describes the energy exchange of the electron with electric field generated by ion channel. In Eqs. (31)–(36), we use the following definitions:

$$\alpha_{12} \equiv k_w c\lfloor\beta_\parallel \mp 2\bar{\Omega}_w I_1(\lambda_0) \pm \bar{\omega}_i^2\lambda_0\beta_w\rfloor, \quad (38)$$

$$\alpha_{14} \equiv k_w c\lfloor\pm\bar{\omega}_i^2\lambda_0 - 2\bar{\Omega}_w\beta_\parallel I_2(\lambda_0) \mp \bar{\omega}_i^2\lambda_0\beta_w^2\rfloor, \quad (39)$$

$$\alpha_{21} \equiv k_w c\lfloor\pm 2\bar{\Omega}_w I_1(\lambda_0) - \beta_\parallel\rfloor, \quad (40)$$

$$\alpha_{23} \equiv k_w c\{-\beta_w + \bar{\Omega}_w[I_2(\lambda_0) - I_0(\lambda_0)]\}, \quad (41)$$

$$\alpha_{25} \equiv k_w c\{\mp\bar{\omega}_i^2 \pm 2\bar{\Omega}_w\beta_w I_1'(\lambda_0) \\ + \bar{\Omega}_w\beta_\parallel[I_2'(\lambda_0) - I_0'(\lambda_0)]\}, \quad (42)$$

$$\alpha_{26} \equiv \frac{k_w c}{\gamma_0}\{\pm\bar{\omega}_i^2\lambda_0 \mp 2\bar{\Omega}_w\beta_w I_1(\lambda_0) \\ - \bar{\Omega}_w\beta_\parallel[I_2(\lambda_0) - I_0(\lambda_0)]\}, \quad (43)$$

$$\alpha_{32} \equiv k_w c\{\pm\bar{\omega}_i^2\lambda_0\beta_\parallel + \bar{\Omega}_w[I_0(\lambda_0) - I_2(\lambda_0)]\}, \quad (44)$$

$$\alpha_{34} \equiv k_w c\{\mp\bar{\omega}_i^2\lambda_0\beta_\parallel\beta_w + 2\bar{\Omega}_w\beta_w I_2(\lambda_0)\}, \quad (45)$$

$$\alpha_{41} \equiv \mp\frac{k_w c}{\gamma_0}, \quad (46)$$

$$\alpha_{43} \equiv -k_w c, \quad (47)$$

$$\alpha_{45} \equiv \pm\beta_\parallel\alpha_{41}, \quad (48)$$

$$\alpha_{52} \equiv \pm k_w c, \quad (49)$$

$$\alpha_{54} \equiv k_w c \lambda_0 \beta_\parallel, \tag{50}$$

$$\alpha_{62} \equiv \mp k_w c \bar{\omega}_i^2 \lambda_0 \gamma_0, \tag{51}$$

$$\alpha_{64} \equiv -\beta_w \alpha_{62}. \tag{52}$$

Differentiating Eqs. (32) and (34) with respect to time and using Eqs. (31), (33), (35), and (36), and after some algebra, we obtain two homogeneous higher-order differential equations as follows:

$$\left(\frac{d^2}{dt^2} + \Omega_1^2\right)\left(\frac{d^2}{dt^2} + \Omega_2^2\right)\begin{pmatrix} \delta\beta_2 \\ \delta\chi \end{pmatrix} \equiv K_1 K_2 \begin{pmatrix} \delta\beta_2 \\ \delta\chi \end{pmatrix}, \tag{53}$$

where

$$\Omega_1^2 \equiv -(\alpha_{21}\alpha_{12} + \alpha_{23}\alpha_{32} + \alpha_{25}\alpha_{52} + \alpha_{26}\alpha_{62}), \tag{54}$$

$$\Omega_2^2 \equiv -(\alpha_{14}\alpha_{41} + \alpha_{34}\alpha_{43} + \alpha_{54}\alpha_{45}), \tag{55}$$

$$K_1 \equiv \alpha_{21}\alpha_{14} + \alpha_{23}\alpha_{34} + \alpha_{25}\alpha_{54} + \alpha_{26}\alpha_{64}, \tag{56}$$

$$K_2 \equiv \alpha_{41}\alpha_{12} + \alpha_{43}\alpha_{32} + \alpha_{45}\alpha_{52}. \tag{57}$$

Operating operator $(d^2/dt^2 + \Omega_1^2)(d^2/dt^2 + \Omega_2^2)$ on $\delta\dot{\beta}_1$, $\delta\dot{\beta}_3$, $\delta\dot{\lambda}$, and $\delta\dot{\gamma}$ yields

$$\frac{d}{dt}\left(\frac{d^2}{dt^2} + \Omega_1^2\right)\left(\frac{d^2}{dt^2} + \Omega_2^2\right)\begin{pmatrix} \delta\beta_1 \\ \delta\beta_3 \\ \delta\lambda \\ \delta\gamma \end{pmatrix} = K_1 K_2 \begin{pmatrix} \delta\beta_1 \\ \delta\beta_3 \\ \delta\lambda \\ \delta\gamma \end{pmatrix}. \tag{58}$$

The stability of orbits can be determined as follows. All variables oscillate with the same frequency ω and are represented by

$$\begin{pmatrix} \delta\beta_1 \\ \delta\beta_2 \\ \delta\beta_3 \\ \delta\chi \\ \delta\lambda \\ \delta\gamma \end{pmatrix} = \begin{pmatrix} A_1 \\ A_2 \\ A_3 \\ A_4 \\ A_5 \\ A_6 \end{pmatrix} e^{i\omega t}. \tag{59}$$

Substituting Eq. (59) into either Eqs. (53) or (58) yields

$$\omega^4 - (\Omega_1^2 + \Omega_2^2)\omega^2 + \Omega_1^2\Omega_2^2 - K_1 K_2 = 0. \tag{60}$$

Equation (60) is the characteristic equation of the system and is quadratic in ω^2. Therefore the system will be stable if both roots of this equation are real and positive. Thus the stability conditions for electron orbits can be written as

$$(\Omega_1^2 - \Omega_2^2)^2 + 4K_1 K_2 > 0, \tag{61}$$

$$\Omega_1^2 + \Omega_2^2 > 0, \tag{62}$$

$$\Omega_1^2\Omega_2^2 - K_1 K_2 > 0. \tag{63}$$

IV. GAIN EQUATION

Now consider the electromagnetic radiation copropagating with the electron in the free-electron laser interaction region. The electric and magnetic radiation fields may be represented by

$$\mathbf{E}_r = E_r(\hat{\mathbf{e}}_x \cos\xi - \hat{\mathbf{e}}_y \sin\xi), \tag{64}$$

$$\mathbf{B}_r = E_r(\hat{\mathbf{e}}_x \sin\xi + \hat{\mathbf{e}}_y \cos\xi), \tag{65}$$

where $\xi \equiv k_r z - \omega_r t + \phi$ is the phase, k_r is the wave number, and ω_r is the angular frequency. In the wiggler rotating frame, the radiation field [Eqs. (64) and (65)] may be written as

$$\mathbf{E}_r = E_r[\hat{\mathbf{e}}_1 \cos(\xi + k_w z) - \hat{\mathbf{e}}_2 \sin(\xi + k_w z)], \tag{66}$$

$$\mathbf{B}_r = E_r[\hat{\mathbf{e}}_1 \sin(\xi + k_w z) + \hat{\mathbf{e}}_2 \cos(\xi + k_w z)]. \tag{67}$$

Using Eqs. (66) and (67), the electron equation of motion for the normalized velocity components in the presence of the radiation fields may be written in the scalar form

$$\frac{d\beta_1}{dt} = -k_w c\{\bar{\omega}_i^2\lambda\cos\chi + \beta_2[2\bar{\Omega}_w I_1(\lambda)\sin\chi - \beta_3]$$
$$- \beta_3\bar{\Omega}_w I_1(\lambda)\sin(2\chi)\} - \frac{eE_r}{m\gamma c}(1 - \beta_3)\cos(\xi + k_w z), \tag{68}$$

$$\frac{d\beta_2}{dt} = -k_w c\{\bar{\omega}_i^2\lambda\sin\chi - \beta_1[2\bar{\Omega}_w I_1(\lambda)\sin\chi - \beta_3]$$
$$+ \beta_3\bar{\Omega}_w[I_0(\lambda) + I_2(\lambda)\cos(2\chi)]\}$$
$$+ \frac{eE_r}{m\gamma c}(1 - \beta_3)\sin(\xi + k_w z), \tag{69}$$

$$\frac{d\beta_3}{dt} = k_w c\bar{\Omega}_w\{\beta_2[I_0(\lambda) + I_2(\lambda)\cos\chi] - \beta_1 I_2(\lambda)\sin(2\chi)\}$$
$$+ \frac{eE_r}{m\gamma c}[\beta_2\sin(\xi + k_w z) - \beta_1\cos(\xi + k_w z)]. \tag{70}$$

Note that the equation of motion for χ and λ are the same as Eqs. (10) and (11), respectively. For solution of Eqs. (68)–(70), we consider that for $\beta_3(\equiv\beta_2)$ close to 1, the last terms in Eqs. (68) and (69) that are due to the transverse optical force acting on electrons may be neglected in comparison with the other terms which are due to the transverse forces of the static wiggler magnetic field and electric field of the ion channel. Thus for β_3 close to 1, Eqs. (68) and (69) are the same as Eqs. (7) and (8), respectively. Therefore, to a very good approximation, the transverse electron velocity components in the presence of the radiation field may be taken as the steady-state solutions [Eqs. (12) and (13)]. Substituting Eqs. (12) and (13) into $\gamma^{-2} = 1 - \beta_1^2 - \beta_2^2 - \beta_3^2$ gives an expression for the normalized axial velocity β_3 in the presence of the radiation field, which may be expanded for $\gamma \gg 1$ and β_3 close to 1 to obtain

$$\beta_3 \cong 1 - \frac{1}{2}\left\{ \gamma^{-2} + \left[\frac{2\bar{\Omega}_w\beta_\parallel^2 I_1(\lambda_0)/\lambda_0}{\bar{\omega}_i^2 \pm 2\bar{\Omega}_w\beta_\parallel I_1(\lambda_0) - \beta_\parallel^2} \right]^2 \right\}. \quad (71)$$

The energy exchange between an electron and the radiation field is given by

$$\dot{\gamma} = -\frac{e}{mc}\boldsymbol{\beta} \cdot \ddot{\mathbf{E}}_r. \quad (72)$$

Substituting Eqs. (12), (13), and (66) into Eq. (72) yields

$$\dot{\gamma} = -\frac{eE_r}{mc}\left(\frac{2\bar{\Omega}_w\beta_\parallel^2 I_1(\lambda_0)/\lambda_0}{\bar{\omega}_i^2 \pm 2\bar{\Omega}_w I_1(\lambda_0)\beta_\parallel - \beta_\parallel^2} \right)$$
$$\times \cos[(k_r + k_w)z - \omega_r t + \phi]. \quad (73)$$

Let the pondermotive phase or electron phase be defined as

$$\psi = (k_r + k_w)z - \omega_r t + \phi. \quad (74)$$

Differentiating twice with respect to time gives

$$\ddot{\psi} = (k_r + k_w)c\dot{\beta}_3. \quad (75)$$

Eliminating $\dot{\beta}_3$ by differentiating Eq. (71) with respect to time and then using Eq. (73) leads to

$$\ddot{\psi} = -\kappa^2 \cos\psi, \quad (76)$$

where

$$\kappa^2 \equiv (k_r + k_w)\frac{eE_r\beta_w}{m\gamma^3}\left[1 - \frac{(\gamma\beta_\parallel P)^2}{R^3} - \frac{SI_1(\lambda_0)}{P^4} \right], \quad (77)$$

$$R \equiv \bar{\omega}_i^2 \pm 2\bar{\Omega}_w\beta_\parallel I_1(\lambda_0) - \beta_\parallel^2, \quad (78)$$

and

$$S = 4\bar{\Omega}_w^2\beta_\parallel^6 R\{(\bar{\omega}_i^2 - \beta_\parallel^2)[\lambda_0 I_1'(\lambda_0) - I_1(\lambda_0)] \mp 2\bar{\Omega}_w\beta_\parallel[I_1(\lambda_0)]^2\}. \quad (79)$$

Equation (76) is the self-consistent pendulum equation describing electron-photon interaction in the presence of a realizable helical wiggler and an ion channel. Using the method used in Ref. 6, Eq. (73) can be written in the form

$$\dot{\gamma} = -\frac{eE_r\beta_w}{mc}\{\cos(\Omega t + \phi) - D\sin(\Omega t + \phi)[\cos(\Omega t + \phi)$$
$$- \cos\phi + \Omega t\sin\phi]\}, \quad (80)$$

where $\Omega \equiv (k_r + k_w)c\beta_\parallel - \omega_r$ and $D \equiv \kappa^2/\Omega^2$. Averaging over all phases ϕ, Eq. (80) becomes

$$\langle\dot{\gamma}\rangle_\phi = \frac{eE_r\beta_w D}{2mc}[\Omega t\cos(\Omega t) - \sin(\Omega t)]. \quad (81)$$

Integrating the above equation over the electron transit time through the wiggler interaction length yields the average change in γ per electron;

$$\langle\Delta\gamma\rangle_\phi = \int_0^r \langle\dot{\gamma}\rangle_\phi dt$$
$$= \frac{eE_r\beta_w D}{2mc\Omega}[\Omega t\sin(\Omega T) + 2\cos(\Omega T) - 2], \quad (82)$$

where $T \equiv L(c\beta_\parallel)^{-1}$ and L is the FEL interaction length. The change in electromagnetic power in one transit is

$$\Delta P_{\text{em}} = -\frac{I}{e}mc^2\langle\Delta\gamma\rangle_\phi, \quad (83)$$

where $I = en_b c\beta_\parallel \cdot$ Area is the average electron beam current and n_b is the electron beam density. Finally, by using Eq. (83) under the assumption that the electrons are near the resonance with the electromagnetic wave [i.e., $\Omega = (k_r + k_w)c\beta_\parallel - \omega_r = 0$], the gain equation becomes

$$G \equiv \frac{\Delta P_{\text{em}}}{P_{\text{em}}} = \frac{8\pi^2 e^2 n_b L^3}{m\gamma c^2\beta_\parallel^3\lambda_w}\beta_w^2 F(\bar{\omega}_i)\mathsf{g}(\Omega T). \quad (84)$$

Here, $P_{\text{em}} \equiv c(E_r^2/4\pi) \cdot$ Area is the electromagnetic power,

$$F(\bar{\omega}_i) \equiv 1 - \frac{(R + \beta_\parallel^2)P^2\gamma^2 + SR^3P^{-4}I_1(\lambda_0)}{(R^2 + P^2\gamma^2)R} \quad (85)$$

and

$$\mathsf{g}(\Omega T) \equiv \frac{2 - 2\cos(\Omega T) - \Omega T\sin(\Omega T)}{(\Omega T)^3} \quad (86)$$

is called the normalized gain equation. Equation (84) is the gain equation for a free-electron laser with realizable helical wiggler and ion-channel guiding in the low-gain-per-pass limit.

In the limit $\lambda \to 0$, Eq. (84) reduces to

$$G^{\text{id}} = \frac{8\pi^2 e^2 n_b L^3}{m\lambda_w c^2(\gamma\beta_\parallel)^3} \cdot \frac{\alpha_w^2\beta_\parallel^4}{(\bar{\omega}_i^2 - \beta_\parallel^2)^2}F^{\text{id}}(\bar{\omega}_i)\mathsf{g}(\Omega T), \quad (87)$$

where $\alpha_w \equiv eB_w/(mk_w c^2)$ is the wiggler parameter, and

$$F^{\text{id}}(\bar{\omega}_i) \equiv 1 - \frac{\alpha_w^2\bar{\omega}_i^2\beta_\parallel^4}{(\bar{\omega}_i^2 - \beta_\parallel^2)^3 + \alpha_w^2\beta_\parallel^4(\bar{\omega}_i^2 - \beta_\parallel^2)}. \quad (88)$$

Equation (88) is exactly the same as the gain equation in Ref. 6 for an idealized helical wiggler and ion-channel guiding.

V. NUMERICAL STUDY OF ORBITS AND GAIN

A numerical study of the electron orbits and gain in a free-electron laser with realizable helical wiggler in the presence of ion-channel guiding has been made. The normalized axial velocity $\beta_\parallel$, the function Φ which determines the mass regimes, and the absolute value of the normalized gain $|G/G_0|$ have been computed using Eqs. (24), (28), and (84), respectively, where $G_0 \equiv 8\pi^2 e^2 n_b L^3\bar{\Omega}_w^2/(m\gamma c^2\beta_\parallel^3\lambda_w)$. For calculation of the gain, the normalized axial velocity $\beta_\parallel$ was taken to be close to 1 (i.e., $\beta_\parallel > 0.9$). The graph of the normalized axial velocity $\beta_\parallel$ as a function of the normalized ion-channel frequency $\bar{\omega}_i$ is shown in Fig. 1. Group-I and group-II orbits are defined by Eqs. (22) and (23), respectively. In this figure, the dashed lines indicate unstable orbits. For stable group-I orbits, $\beta_\parallel$ decreases gradually with in-
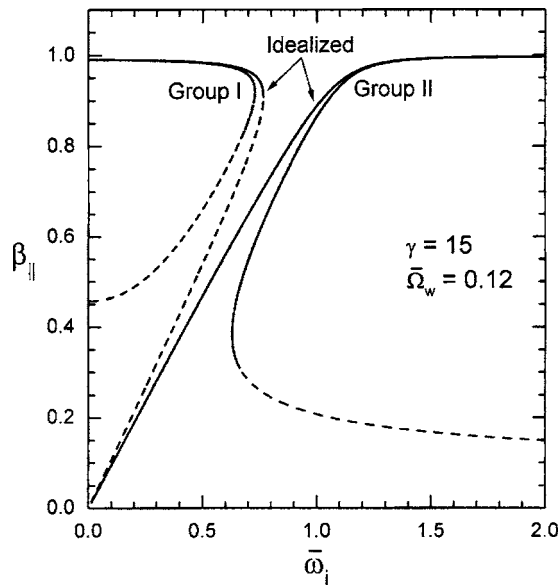
FIG. 1. Graph of the normalized axial velocity as a function of the normalized ion channel frequency for both the realizable wiggler and idealized wiggler. The dashed lines indicate the unstable orbits.

FIG. 3. Graph of the absolute value of the normalized gain as a function of the normalized ion-channel frequency for both realizable wiggler (solid lines) and idealized wiggler (dashed lines).

creasing normalized ion-channel frequency $\bar{\omega}_i$ until the curve terminates at the point of orbital instability. For the parameters chosen in this figure, orbital instability occurs at $\bar{\omega}_i$ =0.73. For stable group-I orbits, because of the conservation of electron energy, the transverse velocity increases with increasing ion-channel frequency. The idealized orbits are also shown here for comparison. The main difference between the results found for the realizable helical wiggler and idealized wiggler is that, in the realizable one, there is an additional branch of unstable orbits (for group II). Also, there are no group-II orbits for $\bar{\omega}_i < 0.63$ (for the parameters chosen in this figure). The Φ function that determines the rate of change of axial velocity with energy is shown in Fig. 2 for

stable branches of group-I and group-II orbits (solid lines). For stable group-I orbits, Φ increases monotonically and exhibits a singularity at the transition to orbital instability. For stable group-I orbits, because of $\Phi > 0$, there is a positive mass regime. For stable group-II orbits, there are three mass regimes; a negative mass regime ($\Phi < 0$) for $0.63 \le \bar{\omega}_i < 1.57$, a zero mass regime ($\Phi = 0$) for $\bar{\omega}_i = 1.57$, and a positive mass regime ($\Phi > 0$) for $\bar{\omega}_i > 1.57$. As shown in Fig. 2, for stable group-II orbits, Φ exhibits a singularity at the transition to orbital instability, which is not found for the idealized helical wiggler. Figure 3 shows the absolute value of the normalized gain ($|\bar{G}| = |G/G_0|$) as a function of normalized
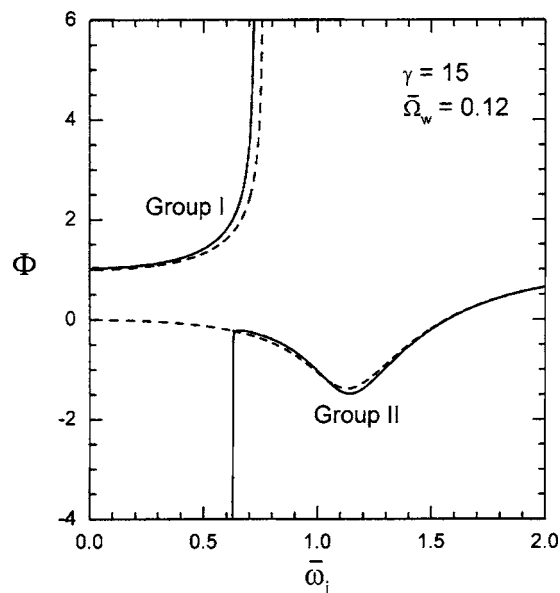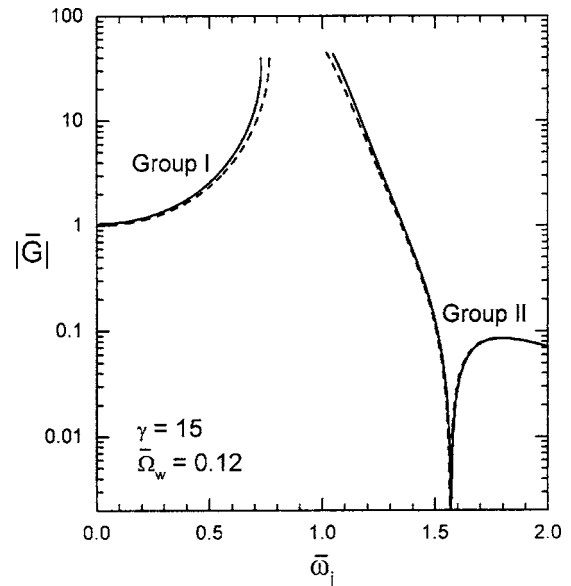

FIG. 2. Graph of Φ as a function of the normalized ion-channel frequency for both realizable wiggler (solid lines) and idealized wiggler (dashed lines).
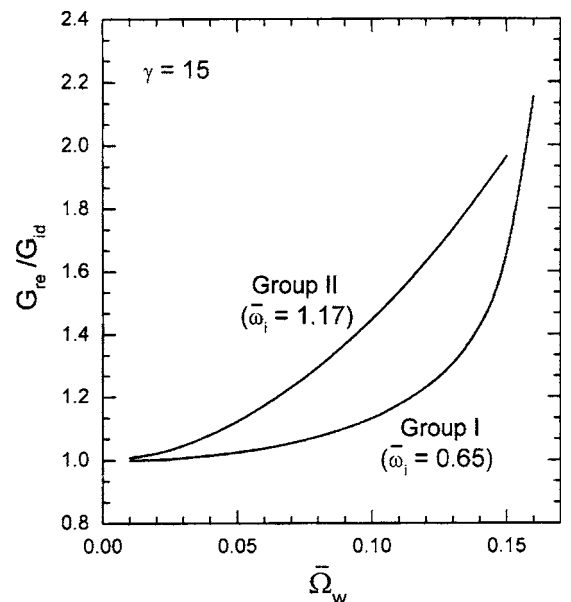

FIG. 4. Graph of the ratio of gain of realizable wiggler to the gain of idealized wiggler G^{re}/G^{id} as a function of the normalized wiggler magnetic field when the normalized ion-channel frequency $\bar{\omega}_i$ is held constant.

ion-channel $\bar{\omega}_i$ for both realizable wiggler (solid lines) and idealized wiggler (dashed lines). For group-I orbits of realizable wiggler (solid lines), the normalized gain increases monotonically from unity at $\bar{\omega}_i=0$ and goes to its maximum ($\equiv 40$) near the resonant ion-channel frequency at the transition point to orbital instability, $\bar{\omega}_i=0.73$. Therefore, the gain enhancement is obtained near the transverse velocity resonance. For group-II orbits of realizable wiggler (solid lines), if $\bar{\omega}_i < 1.05$, the condition $\beta_\parallel > 0.9$ ($\beta_\parallel$ close to 1), as required for derivation of the gain equation, breaks down; for $\bar{\omega}_i \geq 1.05$, the normalized gain is negative and equal to 43 at $\bar{\omega}_i=1.05$ (near the resonant frequency), and goes to zero at $\bar{\omega}_i=1.57$. For $\bar{\omega}_i=1.57$, the normalized gain becomes positive and goes to its maximum (which is less than 1) and then starts decreasing to zero with increasing guiding frequency $\bar{\omega}_i$. As mentioned before, for group-II orbits, the function Φ is negative (negative mass regime) when $\bar{\omega}_i < 1.57$ goes to zero at $\bar{\omega}_i=1.57$ (zero mass regime), and then becomes positive (positive mass regime) when $\bar{\omega}_i > 1.57$. Therefore, the normalized gain G/G_0 is negative in the negative mass regime, zero at zero mass regime, and positive in the positive mass regime. Comparison of the gain of the realizable wiggler (solid lines) with the gain of the idealized wiggler (dashed lines) shows that there is a gain enhancement due to the realizable wiggler relative to the idealized one, particularly near the transverse velocity resonance. For instance, at $\bar{\omega}_i=0.726$ for group-I orbits, $\bar{G}^{\text{re}}=39.73$ and $\bar{G}^{\text{id}}=12.76$ (for parameters used in Fig. 3). As mentioned before in Sec II,

the magnetic field of a realizable wiggler [Eq. (1)] indicates a local minimum on the axis which acts to focus and to confine the beam against the effects of the self fields.[8] The property of the realizable wiggler causes the gain increment relative to the idealized wiggler.

Figure 4 shows the ratio of gain of a realizable wiggler to the gain of an idealized one ($G^{\text{re}}/G^{\text{id}}$) as a function of the normalized wiggler magnetic field $\bar{\Omega}_w$, when the normalized ion-channel frequency $\bar{\omega}_i$ is held constant ($\bar{\omega}_i=0.65$ for group I and $\bar{\omega}_i=1.17$ for group II). As shown in this figure, for both groups, the gain enhancement (relative to the idealized wiggler) increases monotonically with increasing wiggler magnetic field.

[1] K. Takayama and S. Hiramatsu, Phys. Rev. A **37**, 173 (1988).
[2] P. Jha and P. Kumar, IEEE Trans. Plasma Sci. **24**, 359 (1996).
[3] P. Jha and P. Kumar, Phys. Rev. E **57**, 2256 (1998).
[4] M. Esmaeilzadeh, H. Mehdian, and J. E. Willett, Phys. Rev. E **65**, 016501 (2002).
[5] M. Esmaeilzadeh, H. Mehdian, and J. E. Willett, J. Plasma Phys. **70**, 9 (2004).
[6] M. Esmaeilzadeh, H. Mehdian, J. E. Willett, and Y. M. Aktas, Phys. Plasmas **10**, 905 (2003).
[7] M. Esmaeilzadeh, J. E. Willett, and L. J. Willett, "Self-fields in a free-electron laser with helical wiggler and axial magnetic field," J. Plasma Phys. (in press).
[8] H. P. Freund and J. M. Antonsen, Jr., *Principles of Free-Electron Lasers* (Chapman and Hall, London, 1996).
[9] P. Diament, Phys. Rev. A **23**, 2537 (1981).
[10] H. P. Freund and A. K. Ganguly, IEEE J. Quantum Electron. **21**, 1073 (1985).
[11] J. Fajans, D. A. Kirkpatrick, and G. Bekefi, Phys. Rev. A **32**, 3448 (1985).